Magnonic Band Structure in a Skyrmion Magnonic Crystal

Fusheng Ma[1], Yan Zhou[2,3], and Wen Siang Lew[4]

[1]Temasek Laboratories, National University of Singapore, Singapore 119077
[2]York-Nanjing Joint Center for Spintronics and Nano Engineering (YNJC), School of Electronics Science and Engineering, Nanjing University, Nanjing 210093, China
[3]Department of Physics, The University of Hong Kong, Hong Kong
[4]School of Physical and Mathematical Sciences, Nanyang Technological University, Singapore 639798

We present a numerical investigation of the magnonic band structure of spin waves (SWs) in a novel magnonic crystal consisting of a waveguide with a linear array of periodically spaced skyrmions created along its center by micromagnetic simulations. The interfacial Dzyaloshinskii–Moriya interaction (DMI) induced the presence of skyrmions causes a periodical magnetization modulation of the waveguide, which can be dynamically controlled by changing either the strength of the external magnetic field or the period of the skyrmion lattice. The diameters of the skyrmions are highly dependent on the strength of the applied magnetic field, and they can exist for a wide magnetic field range depending on the density of the DMI. The calculated dispersion relation of SWs in the proposed skyrmion magnonic crystal, frequency versus wave vector, exhibits a periodical property, which is the characteristic feature of the band structure of conventional magnonic crystals. Similarly, the calculated magnonic spectra exhibits allowed frequency band and forbidden frequency bandgaps. Our findings could stimulate further exploration on multiple functionalities provided by magnonic crystals based on periodic skyrmion lattices.

Index Terms— **Magnetic skyrmion, magnonic crystals, micromagnetic simulations, spin wave (SW).**

I. Introduction

MAGNETIC skyrmions are vortex-like topologically stable spin textures, whose microscopic magnetic moments are of a whirling configuration and characterized by a finite topological winding number [1]–[4]. They are promising candidates as information carriers for future spintronic devices because of their small size, facile current-driven motion, and topological stability [5]. The controllable nucleation and motion of skyrmions in magnetic nanostructures has been intensively explored which will be essential in the future skyrmionic-spintronic devices for memory, magnetic racetrack, and logic applications [6]–[10]. However, the spin dynamics of either individual skyrmion or skyrmion lattices are rarely studies. Actually, the behavior of magnetic skyrmions is of enormous interest in the emerging field of magnonics as they form a lattice in a self-organized manner whose magnetic properties are periodically modulated [11]–[14]. The periodic modulation of the magnetic properties of the skyrmion lattice is expected to specifically tailor the magnonic band structure of spin waves (SWs) in them. The potential of the skyrmion lattices for spintronics and magnonics is at an initial stage and still needs to be further explored.

In this paper, we propose a novel skyrmion magnonic crystal (SMC). The SMC is based on a perpendicularly magnetized heavy metal/ultra-thin ferromagnet bilayer waveguide with a perpendicular magnetic anisotropy, in which the interfacial symmetry-breaking introduces the presence of interfacial Dzyaloshinskii–Moriya interaction (DMI) [15], [16]. The magnetic periodicity of the waveguide is realized by the presence of spatially periodic array of skyrmions created by the spin current, whose properties are dynamically controllable by the perpendicularly applied magnetic field. The dispersion relation of SW propagation in them, i.e., magnonic band structure is numerically explored. The calculated magnonic spectra exhibit a periodic property with allowed frequency band and forbidden frequency bandgaps, which is similar to that for the conventional magnonic crystals.

Manuscript received March 20, 2015; revised May 25, 2015 and June 3, 2015; accepted June 6, 2015. Date of publication June 10, 2015; date of current version October 22, 2015. Corresponding author: F. Ma (e-mail: fusheng.ma@gmail.com).

Color versions of one or more of the figures in this paper are available online at http://ieeexplore.ieee.org.

Digital Object Identifier 10.1109/TMAG.2015.2443181

II. Simulation Method

The SMC is in the form of an SW waveguide that is assumed to be an ultrathin cobalt (Co) layer on a metallic platinum (Pt) substrate inducing interfacial DMI. The length of the waveguide L is 3000 nm, the width W is 60 nm, and the thickness of the Co layer is 1 nm. The artificial crystal lattice is realized by creating a linear array of equally spaced skyrmions with a period P along the center of the magnonic waveguide. Micromagnetic simulations were performed using the public Object-Oriented Micromagnetic Framework code including the extension module of the DMI [17]–[19]. The uniformly discretized grid was used with the size of the cell $1\times1\times1$ nm^3. The material parameters of the waveguide used in the simulations are listed as follows: 1) the saturation magnetization $M_s = 1.752 \times 10^6$ A/m; 2) the exchange stiffness $A = 2.1 \times 10^{-11}$ J/m; and 3) the perpendicular magnetic anisotropy $K = 0.8$ MJ/m^3 for Co. The intensity of the DMI used in this paper $D = 3$ mJ/m^2, the damping constant $\alpha = 0.01$, and the gyromagnetic ratio $\gamma = 2.211 \times 10^5$ m/As.

A static magnetic field H is perpendicularly applied to the plane of the waveguide along the z-direction. The magnetic periodicity of the waveguide is realized by the presence of spatially periodic array of skyrmions along its center. The system was first relaxed to achieve energy minimum. To excite SWs, a cardinal sin function, $H_y(t) = H_0 \sin(2\pi\omega t)/(2\pi\omega t)$, with $H_0 = 5$ mT and field frequency $\omega = 100$ GHz, was applied locally to a $\Delta x \times \Delta y \times \Delta z = 2 \times 60 \times 1$ nm^3

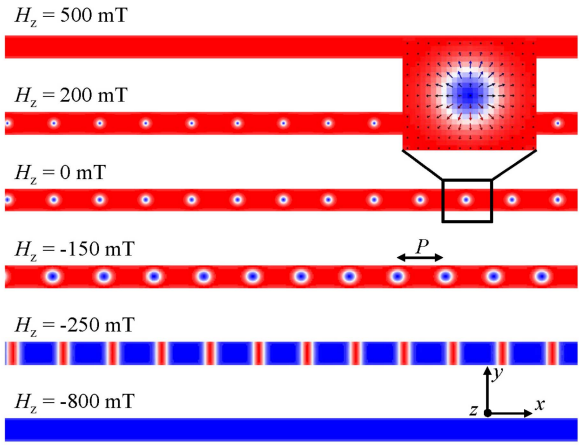

Fig. 1. Spatial distribution of the out-of-plane magnetization component mz of the investigated skyrmion-based magnonic waveguide with a linear array of skyrmions under various perpendicularly applied magnetic fields H. The inset on the top is the pictorial representation of the hedgehog type magnetic skyrmion. The color represents the out-of-plane component of the magnetic moment. It changes from being fully aligned with the $-z$-direction in the center to a complete alignment with the opposite direction in the outer rim. Blue (red) region shows that the z-component of spin is negative (positive), while the white region shows that the spin direction is in-plane. The arrows represent the in-plane component of the magnetic moment.

central section of the magnonic waveguides. In this case, the wave vector k of SWs on the right part is positive, whereas k is negative on the left part. SWs with frequencies ranging from 0 to 100 GHz were thus excited and propagated along the waveguide. The dispersion curves are obtained by performing the Fourier transformation of the out-of-plane magnetization component m_z in space and time with contributions from all the discretized cells.

III. Results

The typical spatial distribution of the out-of-plane magnetization component m_z of the investigated skyrmion-based magnonic waveguide under various perpendicularly applied magnetic fields H is shown in Fig. 1. The initial skyrmion state of the waveguide with the presence of a linear array of skyrmions in its center is simulated under zero magnetic fields. Here, the magnetization of the skyrmion center is oriented along the $-z$-direction, while the magnetization outside the center is oriented in the opposite direction along $+z$. By increasing H from 0 to 500 mT, the skyrmions are gradually shrunk till annihilated as the field direction is opposite to the core of the skyrmions. In contrast, the skyrmions are enlarged by decreasing H from 0 to -800 mT as the field direction is the same as the skyrmion cores. Therefore, the strength of the perpendicularly applied field plays an important role in determining the size of the skyrmions, and hence the periodic magnetization properties of the magnonic waveguide.

The diameters of the skyrmions as a function of the magnetic field strength are shown in Fig. 2 for various DMI constants D. The DMI constant is the necessary parameter for the nucleation of skyrmions in such heavy metal/ferromagnet bilayer structures. As shown in Fig. 2, the value of the D decides the magnetic field range in which the skyrmions can stably exist. For $D = 2.8$ mJ/m^2, the skyrmions can be stabilized in the magnonic waveguide

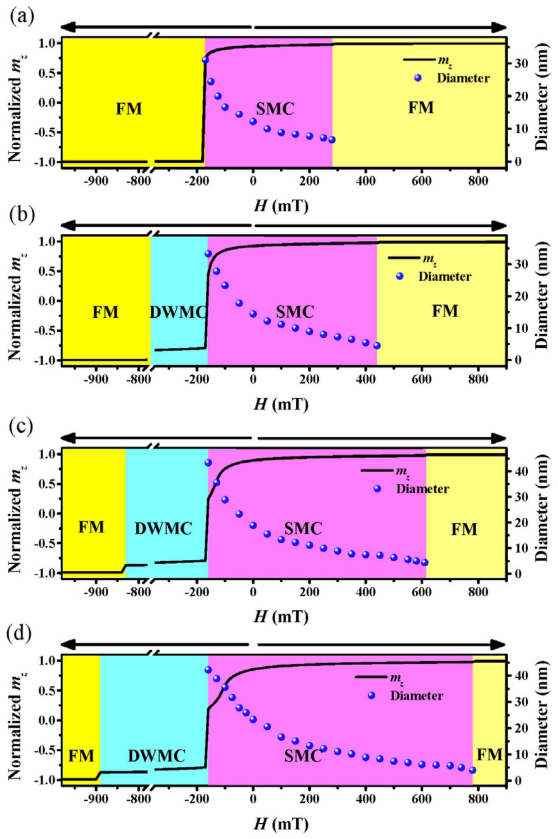

Fig. 2. Normalized out-of-plane magnetization m_z and the skyrmion diameter versus the strength of the magnetic field H applied perpendicular to the plane of the waveguide for various DMI constants D. (a) 2.8, (b) 3.0, (c) 3.2, and (d) 3.4 mJ/m^2.

from -160 to 280 mT with the diameter of the skyrmions decreasing from 31 to 4 nm. When D is increased to 3.0, 3.2, and 3.4 mJ/m^2, the upper field threshold is increased to 440, 610, and 780 mT, respectively. In contrast, the lower magnetic field threshold is the same value of -160 mT. This is because of the limited width $W = 60$ nm of the investigated magnonic waveguide. If the width W of the waveguide is larger, then the lower threshold value would be different. Another interesting result is that there are only three magnetization states for $D = 2.8$ mJ/m^2, i.e., the quasi-uniform out-of-plane ferromagnetic (FM) state in $+z$-direction, the skyrmion magnonic crystal (SMC) state, and the quasi-uniform out-of-plane FM state in $-z$-direction. However, for the other three D values, three are four states: 1) the FM state in $+z$-direction; 2) the SMC state; 3) the domain-wall magnonic crystal (DWMC) state; and 4) the FM state in $-z$-direction. For the calculated magnonic spectra of skyrmion magnonic crystals in this paper, we will take the DMI constant $D = 3.0$ mJ/m^2. As shown in Fig. 2(b), it is observed that the diameters of the skyrmions are continuously shrunk from 15.6 to 4.8 nm by increasing the field from 0 to 440 mT. Above 440 mT, the skyrmions annihilate and the magnetization in the waveguide converts to the FM state in $+z$-direction. When the magnetic field is decreased from 0 to -160 mT from the initial skyrmion state, the diameters of the skyrmions increase from 15.6 to 32.8 nm. Below -160 mT, the skyrmion diameter

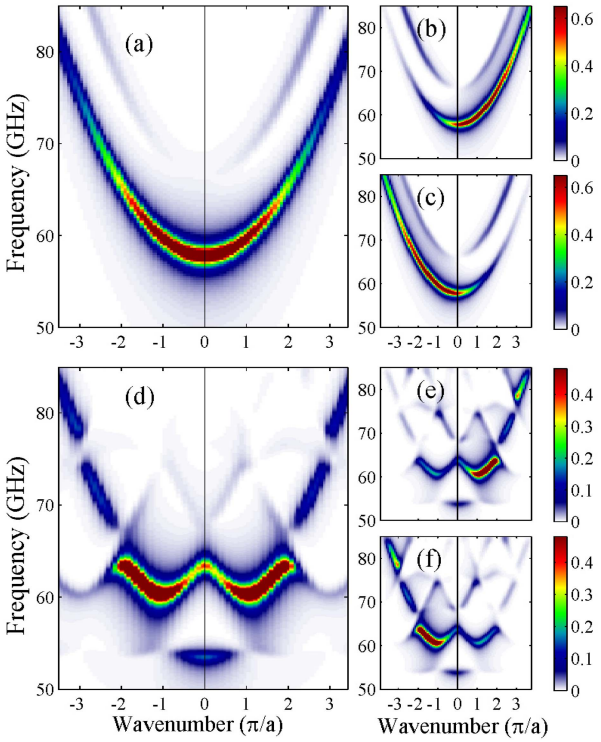

Fig. 3. Dispersion relations of SW propagation in the magnonic waveguide under zero magnetic field: without the presence of a linear array of skyrmions along its (a) center ($y = 30$ nm), (b) bottom edge ($y = 1$ nm), and (c) top edge ($y = 59$ nm), and with the presence of a linear array of skyrmions along its (d) center ($y = 30$ nm), (e) bottom edge ($y = 1$ nm), and (f) top edge ($y = 59$ nm). The dashed lines indicate the Brillouin zone (BZ) boundaries $k_x = n\pi/a$. The intensities of the SWs are represented by the color scale.

becomes larger than the width of the waveguide and they transform into a linear array of equally spaced domain walls (DWs) (Fig. 1). The DW states subsist for a wide field range from -160 to -780 mT. Then the magnetization of the waveguide is fully reversed to the FM state in $-z$-direction. It is needed to be pointed out that the magnetization of the waveguide is also periodically modulated and it can be investigated as domain-wall-based magnonic crystals (DWMCs). It is beyond the scope of this paper and it will be discussed elsewhere.

The numerically calculated dispersion relations of SWs in terms of the frequency versus wave vector for SMC in the FM and skyrmion state are shown in Fig. 3. For the FM state, there is a single parabolic-like dispersion curve and no forbidden frequency band, as shown in Fig. 3(a)–(c). For SWs propagation along the center of the waveguide, their amplitudes with positive wave vector $+k$ and negative wave vector $-k$ are symmetric about the zero wave vector, as shown in Fig. 3(a). However, for SWs propagation along the top and bottom edges of the waveguide, their amplitudes with $+k$ and $-k$ are non-symmetric about the zero wave vector, as shown in Fig. 3(b) and (c). This nonreciprocal character of SW propagation is attributed to the presence of the interfacial DMI [19]–[21]. For the SMC state, the dispersion shows a periodic character of the three dispersion branches up to the third BZ, which is evident from Fig. 3(d). The dispersion curves are observed to be folded and feature bandgaps

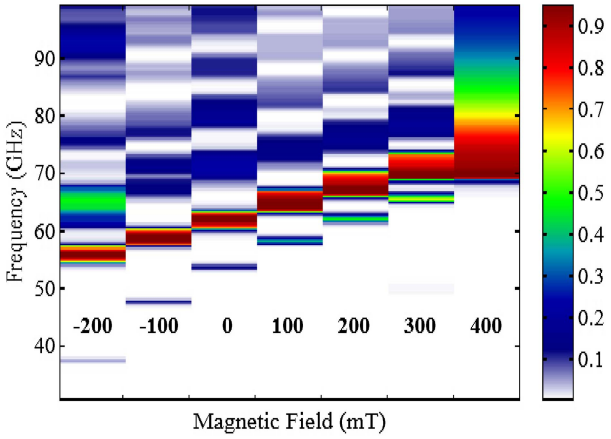

Fig. 4. Magnonic band structure of SW propagation in the magnonic waveguide under the skyrmion state as a function of the strength of the perpendicular applied magnetic field H. The period of the skyrmion is $P = 100$ nm, and the DMI constant $D = 3$ mJ/m^2.

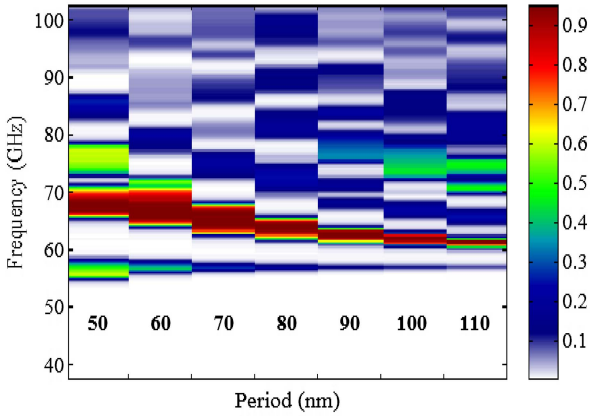

Fig. 5. Magnonic band structure of SW propagation in the magnonic waveguide under the skyrmion state as a function of the period of skyrmions P. The strength of the perpendicular applied magnetic field $H = 60$ mT and the DMI constant $D = 3$ mJ/m^2.

with width of 6, 4, and 2.5 GHz at the BZ boundaries $kx = \pi/a$, $2\pi/a$, and $3\pi/a$, respectively. This is due to the periodic modulation of the magnetic properties along the SW propagation direction induced by the presence of skyrmion lattices. This periodic character is typical of periodic systems such as magnonic band structure for the widely reported magnonic crystals [13]. The observed amplitude nonreciprocity of SWs propagation in the waveguide for the FM state is also observed when the waveguide is in the SMC state, as shown in Fig. 3(e) and (f).

The calculated magnetic field dependence of the magnonic spectra of SWs in the SMC waveguide under the skyrmion state is presented for $P = 100$ mT and $D = 3$ mJ/m^2 in Fig. 4. By increasing the magnetic field from -200 to 400 mT, the width of the bandgaps decrease, while the frequency of the bandgap center increases. This is similar to the observed phenomena for the conventional bicomponent 1-D and 2-D magnonic crystals [22], [23]. For instance, the width of the first bandgap decreases from 17 to 2 GHz, and its center frequencies increase from 46 to 66 GHz when the magnetic field is increased from -200 mT to 300 mT. However, it is

needed to be pointed out that the skyrmions are annihilated with the bandgaps disappear when the magnetic field is higher than 385 mT as shown in Fig. 4 for $H = 400$ mT. For the first allowed frequency band, the width increases from 1.5 to 3 GHz, and its center frequency increases from 37 to 64 GHz.

The effect of the skyrmion lattice period on the magnonic spectra of SWs in the SMC waveguide under the skyrmion state is next discussed. The calculated magnonic spectra are shown as a function of the period P for $H = 60$ mT and $D = 3$ mJ/m^2 in Fig. 5. The band structure of the magnonic spectra is highly affected by the period of the skyrmion lattice. For instance, by increasing the period P from 50 to 110 nm, the width of the first band decreases from 4 to 0.7 GHz, and the frequency of the first band center increases from 56 to 58 GHz. In the meanwhile, the width of the first bandgap decreases from 7 to 2.5 GHz, and its center frequencies decrease from 64 to 60 GHz.

IV. Conclusion

In summary, we have demonstrated a novel magnonic crystal based on a linear array of periodically spaced skyrmions along the magnonic waveguide. The skyrmion-induced spatial variation of the magnetization along the waveguide results in a pronounced modification of SW dispersion, which leads to the appearance of allowed and forbidden bands in its band structure. The properties of the observed magnonic band structure, the width and center frequencies of the bandgaps, can be tuned by changing the size of the skyrmions via adjusting either the strength of the external magnetic field or the period of the skyrmions. Our findings show the potential of the skyrmion lattices as magnonic crystals and could evoke further exploration for their application in the fields of magnonics and spintronics.

Acknowledgment

This work was supported in part by the Temasek Laboratories at National University of Singapore, in part by the Seed Funding Program for Basic Research and Seed Funding Program for Applied Research from the University of Hong Kong, in part by the ITF Tier-3 funding (ITS/171/13), in part by the Research Grant Council - General Research Fund under Grant HKU 17210014, in part by the University Grants Committee of Hong Kong under Contract AoE/P-04/08, and in part by the Singapore National Research Foundation within the Competitive Research Programme under Grant NRF-CRP9-2011-01.

References

[1] U. Al Khawaja and H. Stoof, "Skyrmions in a ferromagnetic Bose–Einstein condensate," *Nature*, vol. 411, pp. 918–920, Jun. 2001.
[2] S. Mühlbauer *et al.*, "Skyrmion lattice in a chiral magnet," *Science*, vol. 323, pp. 915–919, Sep. 2009.
[3] X. Z. Yu *et al.*, "Real-space observation of a two-dimensional skyrmion crystal," *Nature*, vol. 465, no. 7300, pp. 901–904, Jun. 2010.
[4] U. K. Rößler, A. N. Bogdanov, and C. Pfleiderer, "Spontaneous skyrmion ground states in magnetic metals," *Nature*, vol. 442, no. 7104, pp. 797–801, Aug. 2006.
[5] N. Nagaosa and Y. Tokura, "Topological properties and dynamics of magnetic skyrmions," *Nature Nanotechnol.*, vol. 8, no. 12, pp. 899–911, Dec. 2013.
[6] A. Fert, V. Cros, and J. Sampaio, "Skyrmions on the track," *Nature Nanotechnol.*, vol. 8, no. 3, pp. 152–156, Mar. 2013.
[7] J. Sampaio, V. Cros, S. Rohart, A. Thiaville, and A. Fert, "Nucleation, stability and current-induced motion of isolated magnetic skyrmions in nanostructures," *Nature Nanotechnol.*, vol. 8, no. 11, pp. 839–844, Nov. 2013.
[8] J. Iwasaki, M. Mochizuki, and N. Nagaosa, "Current-induced skyrmion dynamics in constricted geometries," *Nature Nanotechnol.*, vol. 8, no. 10, pp. 742–747, Oct. 2013.
[9] L. Sun *et al.*, "Creating an artificial two-dimensional skyrmion crystal by nanopatterning," *Phys. Rev. Lett.*, vol. 110, p. 167201, Apr. 2013.
[10] Y. Zhou and M. Ezawa, "A reversible conversion between a skyrmion and a domain-wall pair in a junction geometry," *Nature Commun.*, vol. 5, Aug. 2014, Art. ID 4652.
[11] V. V. Kruglyak, S. O. Demokritov, and D. Grundler, "Magnonics," *J. Phys. D, Appl. Phys.*, vol. 43, no. 26, p. 264001, Jul. 2010.
[12] A. Khitun, M. Bao, and K. L. Wang, "Magnonic logic circuits," *J. Phys. D, Appl. Phys.*, vol. 43, no. 26, p. 264005, 2010.
[13] B. Lenk, H. Ulrichs, F. Garbs, and M. Münzenberg, "The building blocks of magnonics," *Phys. Rep.*, vol. 507, nos. 4–5, pp. 107–136, 2011.
[14] M. Krawczyk and D. Grundler, "Review and prospects of magnonic crystals and devices with reprogrammable band structure," *J. Phys., Condens. Matter*, vol. 26, no. 12, p. 123202, 2014.
[15] I. Dzyaloshinsky, "A thermodynamic theory of 'weak' ferromagnetism of antiferromagnetics," *J. Phys. Chem. Solids*, vol. 4, no. 4, pp. 241–255, 1958.
[16] T. Moriya, "Anisotropic superexchange interaction and weak ferromagnetism," *Phys. Rev.*, vol. 120, pp. 91–98, Oct. 1960.
[17] M. J. Donahue and D. G. Porter. (1999). *OOMMF User's Guide, version 1.0*. [Online]. Available: http://math.nist.gov/oommf
[18] A. Thiaville, S. Rohart, É. Jué, V. Cros, and A. Fert, "Dynamics of Dzyaloshinskii domain walls in ultrathin magnetic films," *Europhys. Lett.*, vol. 100, no. 5, p. 57002, Dec. 2012.
[19] F. Ma and Y. Zhou, "Interfacial Dzialoshinskii–Moriya interaction induced nonreciprocity of spin waves in magnonic waveguides," *RSC Adv.*, vol. 4, no. 87, pp. 46454–46459, Sep. 2014.
[20] J.-H. Moon *et al.*, "Spin-wave propagation in the presence of interfacial Dzyaloshinskii–Moriya interaction," *Phys. Rev. B*, vol. 88, p. 184404, Nov. 2013.
[21] F. Garcia-Sanchez, P. Borys, A. Vansteenkiste, J.-V. Kim, and R. L. Stamps, "Nonreciprocal spin-wave channeling along textures driven by the Dzyaloshinskii–Moriya interaction," *Phys. Rev. B*, vol. 89, p. 224408, Jun. 2014.
[22] F. S. Ma, H. S. Lim, Z. K. Wang, S. N. Piramanayagam, S. C. Ng, and M. H. Kuok, "Micromagnetic study of spin wave propagation in bicomponent magnonic crystal waveguides," *Appl. Phys. Lett.*, vol. 98, no. 15, p. 153107, 2011.
[23] F. S. Ma *et al.*, "Band structures of exchange spin waves in one-dimensional bi-component magnonic crystals," *J. Appl. Phys.*, vol. 111, no. 6, p. 064326, 2011.